Steady-state exhumation of the European Alps

Matthias Bernet* Department of Geology and Geophysics, Yale University, New Haven, Connecticut 06520-8109, USA
Massimiliano Zattin Dipartimento di Scienze della Terra e Geologico-Ambientali, Università di Bologna, I-40127, Bologna, Italy
John I. Garver Geology Department, Olin Building, Union College, Schenectady, New York 12308-2311, USA
Mark T. Brandon Department of Geology and Geophysics, Yale University, New Haven, Connecticut 06520-8109, USA
Joseph A. Vance Department of Geological Sciences, University of Washington, Seattle, Washington 98195-1310, USA

ABSTRACT

Fission-track grain-age distributions for detrital zircon are used in this study to resolve the late Cenozoic exhumation history of the European Alps. Grain-age distributions were determined for six sandstone samples and one modern river sediment sample, providing a record from 15 Ma to present. All samples can be traced to sources in the Western and Central Alps. The grain-age distributions are dominated by two components, P1 (8–25 Ma) and P2 (16–35 Ma), both of which show steady lag times (cooling age minus depositional age), with an average of 7.9 m.y. for P1 and 16.7 m.y. for P2. These results indicate steady-state exhumation in the source region at rates of ~0.4–0.7 km/m.y. since at least 15 Ma.

Keywords: Alps, steady-state, exhumation, erosion, fission-track.

INTRODUCTION

Previous studies of exhumation in the Alps have focused on reconstructing time-temperature-depth histories for currently exposed bedrock (see synthesis by Hunziker et al. 1992). We explore another approach here, using synorogenic sediments to reconstruct the evolution of surface cooling ages with time. Fission-track dating of detrital zircon is well suited for this approach because individual grains can be dated. Furthermore zircon is widely distributed in typical crustal rocks and is robust during weathering and transport (see review by Garver et al., 1999). We present fission-track grain-age distributions for 7 samples of detrital zircons derived from the Alps since 15 Ma. Approximately 80–100 grains were dated per sample, providing a detailed sampling of the distribution of bedrock cooling ages at the time that the sampled sediment was eroded from its source. These data are used to examine the late Cenozoic evolution of exhumation rates in the Alps.

LAG TIME

In orogenic settings, closure of low-temperature chronometers is commonly related to exhumation-related cooling caused by erosion or normal faulting. The lag time of a dated detrital mineral, defined as the amount of time between closure and deposition, provides a measure of the rate of exhumation. The lag time concept is illustrated in Figure 1B. At a closure depth Z_C, zircons pass through the closure temperature T_C and fission tracks are retained. Regional exhumation causes the zircons to move toward the surface where they are eroded at time t_e. Brandon et al. (1998) and Garver et al. (1999) summarized how Z_C for the zircon fission-track system varies as a function of erosion rate. Their calculations are based on a one-dimensional steady-state solution that accounts for the advection of heat and the influence of cooling rate on T_C. Relevant parameters for the European Alps, such as the initial thermal gradient, surface temperature, and crustal thermal diffusivity, are similar to those used in the Himalayan example in Garver et al. (1999). The model calculation predicts $T_C \approx 240–250$ °C for an exhumation rate of 0.5–1 km/m.y., which agrees with Hur-

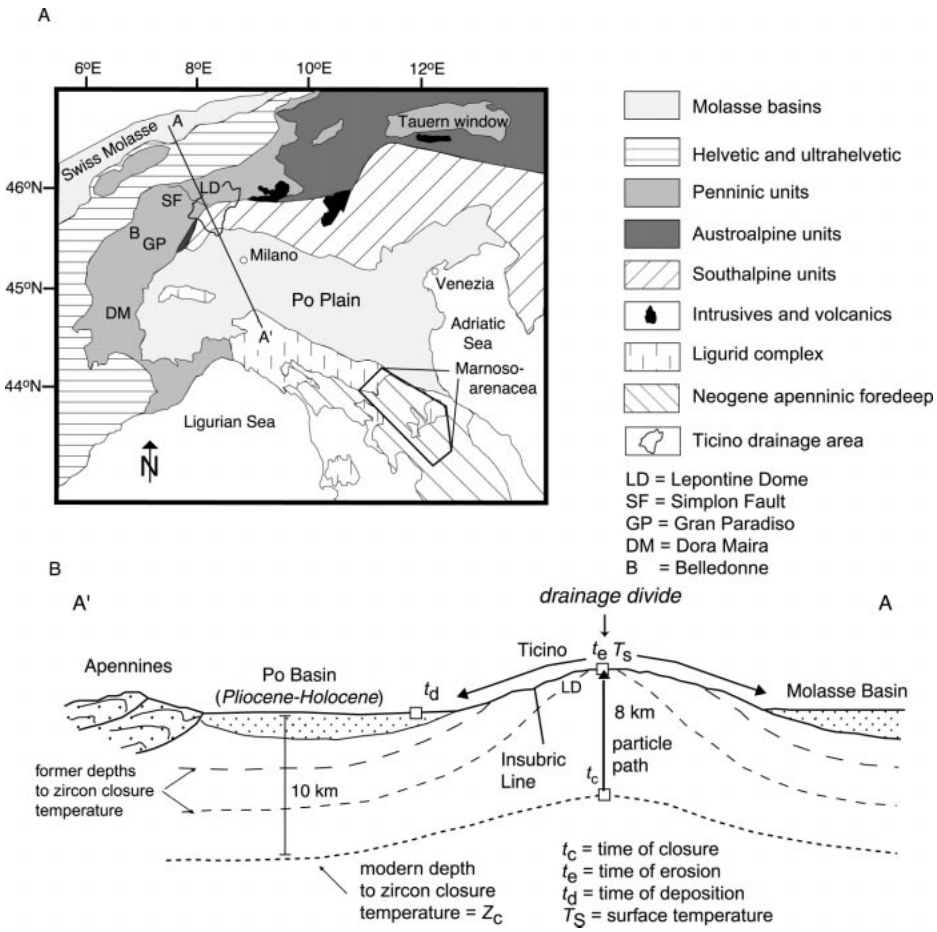

Figure 1. A: Simplified tectonic map of Alps and northern Apennine showing the study area. B: Lag time concept is illustrated using schematic profile (A–A′) through central Alps and adjacent sedimentary basins. Stippled line shows the zircon fission-track closure depth Z_C, where zircons cool through the effective fission-track closure temperature T_C at time t_c. Zircons reach the surface at time t_e and are transported and finally deposited in basin at time t_d.

*E-mail: matthias.bernet@yale.edu.

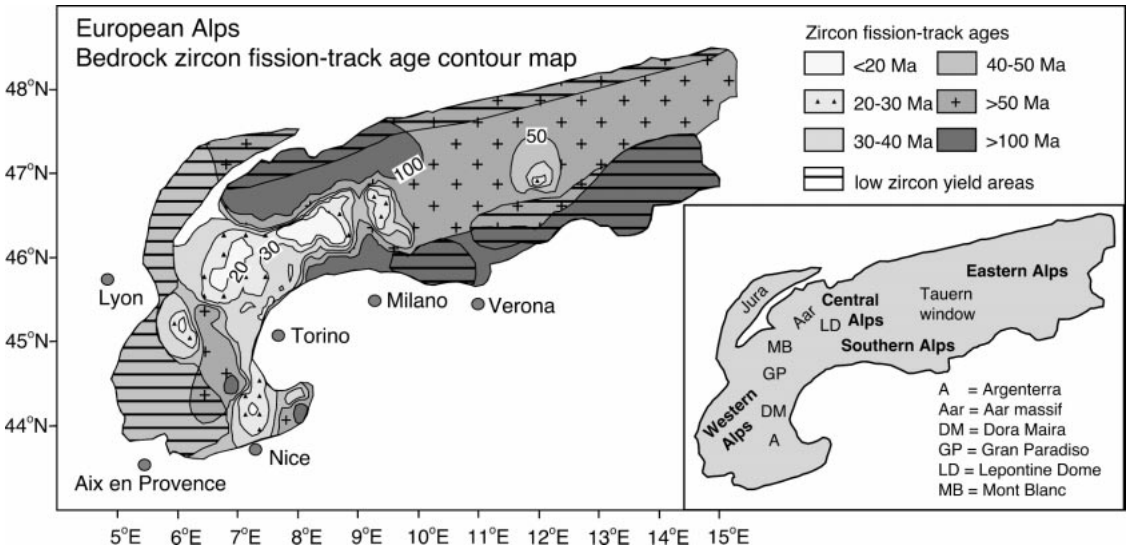

Figure 2. Contour map of zircon fission-track bedrock ages for the European Alps (see text for details). Only broad features are shown in the eastern Alps, southwest part of western Alps, and Jura Mountains because of sparse data coverage.

ford's (1986) field-based estimate for the central Alps. A typical value for Z_C for the central Alps is 5 km. We assume that most of the lag time is spent exhuming the rocks from Z_C. Sedimentary transport at the surface is negligible in comparison (e.g., Brandon and Vance, 1992).

Convergent orogenesis can be divided into idealized phases of construction, steady state, and decay (Jamieson and Beaumont, 1989). The constructional phase involves the growth of topography and an increase in erosion rates, which would be represented in the stratigraphic record by an upsection decrease in lag time. In some cases, the erosional outflux may become large enough to balance the accretionary flux into the orogen. This steady-state phase would be recorded by a stratigraphic interval where lag time remained approximately constant. When convergence stops, the orogen moves into a decay phase, marked by a reduction in topography and a decrease in erosion rates. The decay phase would be recorded by an upsection increase in lag time.

Tectonic exhumation by normal faulting can also influence lag times. If tectonic exhumation is persistent over millions of years, we might expect to see upsection changes in lag time similar to those outlined above for erosional exhumation. An important distinction is that tectonic exhumation does not produce sediment. Thus, a change in the rate of tectonic exhumation will cause a change in lag time, but no direct changes in the flux of eroded sediment.

Alternatively, if tectonic exhumation were rapid and short lived, as is commonly proposed for cases of orogenic collapse, then the grain-age distributions would show an abrupt upsection decrease in lag time. Rapid normal faulting would allow the exhumed footwall to quench to a nearly constant cooling age, extending down to the closure depth. This source region would deliver a relatively constant source of grain ages (static peak of Brandon and Vance, 1992) until erosion had stripped away a thickness equal to the closure depth. The grain-age component from this source would show a steadily increasing lag time, with the increase equal to the amount of time since the exhumation event.

The upsection change in lag time recorded in sediments derived from an active volcanic source might appear similar to that produced by rapid normal faulting. Regional geologic relationships and sedimentary petrography are usually successful in distinguishing between volcanism and rapid exhumation.

TECTONIC SETTING

The Central and Western Alps formed by Cretaceous to present convergence between a subducting European plate and an overriding Adriatic plate (e.g., Frisch, 1979; Platt, 1986). Continental collision started in the Eocene, and led to development of a subaerial orogenic wedge. Surface exposures of the Alpine metamorphic core record peak conditions ca. 35–30 Ma in the Central Alps (Steck and Hunziker, 1994). There was almost no magmatism associated with Alpine convergence. The only significant event was the emplacement of the Periadratic intrusions ca. 33–28 Ma. Siliciclastic sediments of that age show significant volcanogenic detritus (e.g., lower Oligocene Taveyannaz sandstone). Other than this example, sediments derived from the Alps show little to no volcanic influence.

The present pattern of exhumation in the Alps is illustrated in Figure 2, which shows a contour map of bedrock cooling ages compiled from approximately 205 zircon fission-track ages[1]. The youngest ages are associated with the Central Alps. Large volumes of synorogenic sediment provide clear evidence that erosion was an important exhumation process in the Alps (England, 1981). More recent work has demonstrated the importance of tectonic exhumation in the Alps (e.g., Simplon fault: Mancktelow, 1992; Turba mylonite: Nievergelt et al., 1996; Tauern window: Selverstone, 1985; Ratschbacher et al., 1991).

FISSION-TRACK SAMPLES AND RESULTS

Our samples come from 6 localities in the Miocene Marnoso-Arenacea Formation of the Northern Apennines, Italy, and from modern sediments from the lower reach of the Ticino River, which drains the source area for the Marnoso-Arenacea Formation (Fig. 1A). All sediments have an arkosic composition. Zircons are generally subhedral to rounded. Depositional ages are based on biostratigraphy, and are generally known to ± 1 m.y.

As summarized by Ricci Lucchi (1986), the lower part of the Marnoso-Arenacea Formation(<5 Ma) records a flysch stage of deposition in a deep marine foredeep that bordered the east side of an active but otherwise submerged Apennine convergent wedge. Heavy mineral assemblages and paleocurrent directions indicate sedimentary sources in the Central and Western Alps (Gandolfi et al., 1983;

[1]GSA Data Repository item 20019, Zircon fission-track ages of the European Alps, is available on request from Documents Secretary, GSA, P.O. Box 9140, Boulder, CO 80301-9140, editing@geosociety.org, or at www.geosociety.org/pubs/ft2001.htm.

TABLE 1. DETRITAL ZIRCON FISSION-TRACK DATA

Sample	Approximate depositional age (Ma)	N	P1	P2	P3	P4
Ticino River	0	95	8.6 ± 1.4 15.3% 8.6	15.6 ± 1.5 56.5% 15.6	25.6 ± 4.8 19.8% 25.6	140.1 ± 20.1 8.4% 140.1
1	7.5	102	15.2 ± 1.5 39.8% 7.7	24.7 ± 2.2 51.1% 17.2	—	106.7 ± 13.7 9.1% 99.2
2	12.0	102	20.4 ± 1.7 49.2% 8.4	34.2 ± 3.6 25.4% 22.2	69.5 ± 8.1 16.8% 57.5	131.2 ± 20.6 8.6% 119.2
3	12.5	105	18.9 ± 2.4 29.3% 6.4	28.8 ± 3.2 44.3% 16.3	51.7 ± 6.0 14.0% 38.8	115.6 ± 14.8 12.4% 103.1
4	13.8	78	19.5 ± 2.5 28.2% 5.7	27.7 ± 4.2 39.8% 13.9	51.7 ± 12.4 8.7% 37.9	94.9 ± 14.6 15.9% 81.1
5	13.9	101	20.7 ± 3.6 33.4% 6.8	29.9 ± 4.9 50.0% 16.0	49.9 ± 8.8 9.8% 36.0	114.1 ± 20.6 6.7% 100.2
6	15.0	85	23.5 ± 2.1 35.1% 8.5	—	43.9 ± 4.5 24.3% 28.9	110.6 ± 9.6 40.6% 95.6

Note: N is the total number of grains counted; binomial fitted peak ages (Galbraith and Green, 1990) are given in Ma with a 95% confidence interval. The relative size of the specific peak is in percent, and the lag time in m.y. The depositional age is known to ±1 Ma and lag time is calculated by cooling age minus depositional age. Sample treatment is described in Garver et al. (2000).

Valloni and Zuffa, 1984; Cibin et al., 2000). Sandstones with local Apennine sources are present, but they are restricted to rare isolated beds that are easily distinguished by their petrographic composition and a difference in paleocurrent directions (Gandolfi et al., 1983).

Grain-age distributions were decomposed into significant components or peaks using the binomial peak-fitting method (Table 1). Errors are cited at the 95% confidence level. The grain-age distributions are generally dominated by two young peaks, P1 and P2, which are the focus of our analysis here. Older peaks are present but they generally represent <15% of the distribution. P1 varies from 8.6 to 23.5 Ma and P2 from 15.6 to 34.2 Ma (Table 1) but both show nearly constant lag times (Fig. 3).

DISCUSSION

Test for Steady State

Changes in peak age t_c with depositional age t_d can be approximated by a linear relationship, $t_c = A + B\,t_d$ where A and B are fit parameters. Conversion to lag time gives ($t_c - t_d$) $= A + (B - 1)\,t_d$, which shows that A is the present lag time and ($B - 1$) is the change in lag time with depositional age. Thus, the upsection trends in lag time discussed above can be represented by B, with $B < 1$ associated with construction, $B > 1$ with decay, and $B = 1$ with steady state. The linear relationship fits the P1 data well ($R^2 = 0.96$); the residuals are the same size as the uncertainties of the peak ages (reduced $\chi^2 = 1.04$). The best-fit estimate of $B = 0.92 \pm 0.128$ (2 standard error) indicates a steady-state trend. The average lag time is 7.9 m.y. (determined at midpoint of the data distribution).

The linear relationship provides a reasonable fit for the P2 data ($R^2 = 0.86$). The residuals show no systematic variations. Their large size (reduced $\chi^2 = 2.87$) indicates other sources of variance in addition to those related to fission-track measurement of age. The best-fit estimate of $B = 1.13 \pm 0.185$ (2 standard error) is also consistent with a steady-state trend. The average lag time is 16.7 m.y.

Ideally, during steady-state exhumation, the relative sizes of peaks should remain constant. The ratio of peak sizes for P1 and P2 are similar for 4 out of 7 of our samples. We note, however, that lag times provide an estimate of exhumation rate averaged over the lag time (>5 m.y.), whereas the relative peak size is controlled by short-term erosion rates with an averaging constant much less than 1 m.y. We emphasize here the lag time estimates of exhumation rate because they are more relevant to the long-term evolution of the orogen.

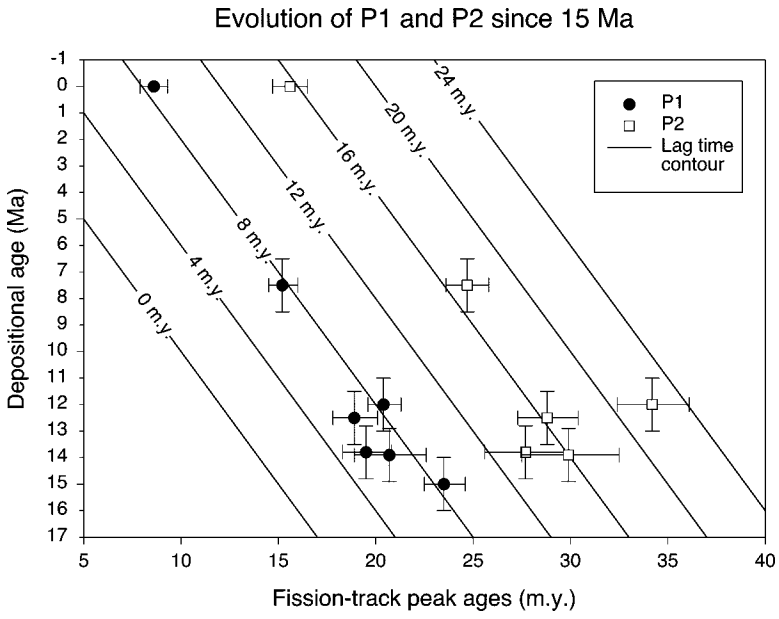

Figure 3. Plot showing the evolution with time of the P1 and P2 component ages. Contours show lines of constant lag time. Error bars show ±1 standard error for peak ages and ±1 m.y. uncertainty for depositional ages.

Source Areas

The contour map (Fig. 2) provides a basis for resolving where the P1 and P2 zircons came from. A viable source area for a component must have a modern zircon fission-track age that is equal to the estimated lag time of the component.

Our P1 ages indicate that the source of these zircons must have a modern bedrock age ca. 8 Ma. This requirement restricts our search to two closely spaced areas in the Alps: (1) the Pennine front in the Aar Massif region (Seward and Mancktelow, 1994), and (2) the Lower Pennine nappes of the Lepontine Dome in the footwall of the Simplon fault (Hunziker et al., 1992; Seward and Mancktelow, 1994). The P1 component is present in our oldest samples, which indicates that by ca. 15 Ma young reset zircons were already eroding from this source.

The modern age of the P2 source is estimated to be ca. 15–20 Ma. In the Central Alps, candidates include the southern and eastern parts of the Lepontine Dome (Hurford, 1986; Hunziker et al., 1992) and the hanging wall of the Simplon fault and in the Western

Alps the Pennine front in the Mont Blanc–Belledonne Massif region (Seward and Mancktelow, 1994; Fügenschuh et al., 1999).

Comparison with Bedrock Studies

The lag time versus erosion rate relationship from Garver et al. (1999) predicts an approximate exhumation rate of ~0.7 km/m.y. for P1 and ~0.4 km/m.y. for P2. These rates are similar to those estimated by the modeling study of the Simplon normal fault by Grasemann and Mancktelow (1993). The youngest cooling ages in the Central Alps occur in the footwall of the Simplon normal fault. Part of the Ticino drainage is eroding the Simplon fault footwall. Grasemann and Mancktelow (1993) indicate a short interval of rapid normal faulting from 18 to 15 Ma with fast rates of tectonic exhumation of the footwall, ~4.6 km/m.y, followed by slower normal faulting from 15 Ma to at least 3 Ma. After 15 Ma, the total exhumation rates were estimated to be 0.6 km/m.y. in the footwall and 0.4 km/m.y. in the hanging wall, which matches the rates estimated for P1 and P2. Grasemann and Mancktelow (1993) attribute the difference in exhumation rates between the footwall and hanging wall to a regional erosion rate of 0.4 km/m.y. and a 0.2 km/m.y. rate of tectonic exhumation for the footwall.

CONCLUSIONS

Detrital zircon fission-track grain ages with depositional ages ranging from 15 to 0 Ma indicate steady lag times for the most rapidly eroding sources. This result indicates that the Alps were being exhumed at a steady rate, and that sediments delivered from Alpine sources came from areas where zircon fission-track ages were set by a combination of tectonic and erosional cooling. Exhumational steady state has been observed in some modern orogens, such as Taiwan (Dahlen and Suppe, 1988), the Southern Alps of New Zealand (Adams, 1980), and northern Cascadia in the northwestern United States (Brandon et al., 1998). Erosion dominates exhumation in those cases. The Alps appear to be another example where erosion and tectonic exhumation are operating together in an approximately steady-state fashion.

ACKNOWLEDGMENTS

This research was supported by a GSA student grant (Bernet), a research grant from the Italian Science Foundation (MURST ex-40% 1997 to Zattin), a National Science Foundation grant (EAR-9614730 to Garver) and the Union College Faculty Research Fund (Garver). Neutron irradiation was subsidized by the Reactor Use Sharing Program (United States Department of Energy) granted to the Oregon State University Nuclear Reactor. We thank Douglas Burbank, Niels Hovius, and Uwe Ring for critical reviews.

REFERENCES CITED

Adams, J., 1980, Contemporary uplift and erosion of the Southern Alps, New Zealand: Geological Society of America Bulletin Part II, v. 91, p. 1–114.

Brandon, M.T., and Vance, J.A., 1992, New statistical methods for analysis of fission track grain-age distributions with applications to detrital zircon ages from the Olympic subduction complex, western Washington State: American Journal of Science, v. 292, p. 565–636.

Brandon, M.T., Roden-Tice, M.K., and Garver, J.I., 1998, Late Cenozoic exhumation of the Cascadia accretionary wedge in the Olympic Mountains, northwest Washington State: Geological Society of America Bulletin, v. 110, p. 985–1009.

Cibin, U., Spadafora, E., Zuffa, G.G., and Castellarin, A., 2001, Continental collision history from arenites of episutural basins in the northern Apennines, Italy: Geological Society of America Bulletin, v. 113 (in press).

Dahlen, F.A., and Suppe, J., 1988, Mechanics, growth, and erosion of mountain belts, *in* Clark, S.P., et al., eds., Processes in continental lithospheric deformation: Geological Society of America Special Paper 218, p. 161–178.

England, P., 1981, Metamorphic pressure estimates and sediment volumes for the Alpine orogeny: An independent control on geobarometers?: Earth and Planetary Science Letters, v. 56, p. 387–397.

Frey, M., Desmons, J., and Neubauer, F., 1999, The new metamorphic map of the Alps: Schweizerische Mineralogische und Petrographische Mitteilungen, v. 79, p. 1–5.

Frisch, W., 1979, Tectonic progradation and plate tectonic evolution of the Alps: Tectonophysics, v. 60, p. 121–139.

Fügenschuh, B., Loprieno, A., Ceriani, S., and Schmid, S.A., 1999, Structural analysis of the Subbriançonnais and Valais units in the area of Moûtiers (Savoy, Western Alps): Paleogeographic and tectonic consequences: International Journal of Earth Sciences, v. 88, p. 201–218.

Galbraith, R.F., and Green, P.F., 1990, Estimating the component ages in a finite mixture: Nuclear Tracks and Radiation Measurements, v. 17, p. 197–206.

Gandolfi, G., Paganelli, L., and Zuffa, G.G., 1983, Petrology and dispersal pattern in the Marnoso-arenacea Formation (Miocene, Northern Apennines): Journal of Sedimentary Petrology, v. 53, p. 493–507.

Garver, J.I., Brandon, M.T., Roden-Tice, M.K., and Kamp, P.J.J., 1999, Exhumation history of orogenic highlands determined by detrital fission track thermochronology, *in* Ring, U., et al., eds., Exhumation processes: Normal faulting, ductile flow, and erosion*:* Geological Society [London] Special Publication 154, p. 283–304.

Garver, J.I., Brandon, M.T., Bernet, M., Brewer, I., Soloviev, A.V., Kamp, P.J.J., and Meyer, N., 2000, Practical consideration for using detrital zircon fission track thermochronology for provenance, exhumation studies, and dating sediments, *in* International Conference on Fission Track Dating and Thermochronology, 9th: Geological Society of Australia Abstract Series, v. 58, p. 109–111.

Grasemann, B., and Mancktelow, N.S., 1993, Two-dimensional thermal modelling of normal faulting: The Simplon fault zone, Central Alps, Switzerland: Tectonophysics, v. 225, p. 155–165.

Hunziker, J.C., Desmond, J., and Hurford, A.J., 1992, Thirty-two years of geochronological work in the Central and Western Alps: A review on seven maps: Memoire de Geologie (Lausanne), v. 13, p. 1–59.

Hurford, A.J., 1986, Cooling and uplift patterns in the Lepontine Alps, south central Switzerland and an age of vertical movement on the Insubric fault line: Contributions to Mineralogy and Petrology, v. 92, p. 413–427.

Jamieson, R., and Beaumont, C., 1989, Deformation and metamorphism in convergent orogens; a model for uplift and exhumation of metamorphic terrains, *in* Daly, J., et al., eds., Evolution of metamorphic belts: Geological Society of London Special Publication 43, p. 117–129.

Mancktelow, N.S., 1992, Neogene lateral extension during convergence in the Central Alps: Evidence from interrelated faulting and backfolding around the Simplonpass (Switzerland): Tectonophysics, v. 215, p. 295–317.

Nievergelt, P., Liniger, M., Froitzheim, N., and Maehlmann, R.F., 1996, Early to mid Tertiary crustal extension in the central Alps, the Turba mylonite zone (eastern Switzerland): Tectonics, v. 15, p. 329–340.

Platt, J.P., 1986, Dynamics of orogenic wedges and the uplift of high-pressure metamorphic rocks: Geological Society of America Bulletin, v. 97, p. 1037–1053.

Ratschbacher, L., Frisch, W., Linzer, H.G., and Merle, O., 1991, Lateral extrusion in the Eastern Alps, structural analysis: Tectonics, v. 10, p. 257–271.

Ricci Lucchi, F., 1986, The foreland basin system of the Northern Apennines and related clastic wedges: A preliminary outline: Giornale di Geologia, ser. 3, v. 48, p. 165–185.

Selverstone, J., 1985, Constraints on imbrication, metamorphism, and uplift in the SW Tauern Window, Eastern Alps: Tectonics, v. 4, p. 687–704.

Seward, D., and Mancktelow, N.S., 1994, Neogene kinematics of the central and western Alps: Evidence from fission track dating: Geology, v. 22, p. 803–806.

Steck, A., and Hunziker, J., 1994, The Tertiary structural and thermal evolution of the central Alps—Compressional and extensional structures in an orogenic belt: Tectonophysics, v. 238, p. 229–254.

Valloni, R., and Zuffa, G.G., 1984, Provenance changes for arenaceous formations of the northern Apennines, Italy: Geological Society of America Bulletin, v. 95, p. 1035–1039.

Manuscript received June 16, 2000
Revised manuscript received October 9, 2000
Manuscript accepted October 9, 2000

Printed in USA

Zircon fission track ages of the European Alps

Data for contour plot

sample	Longitude degrees east	Latitude degrees north	zircon [Ma]	+/- [Ma]	altitude [m]	Location	lithology	author
BC1*	6.886	44.336	76.1	3.8	n/a	n/a	n/a	Bigot-Cormier et al. (1999)
BC2*	6.919	44.323	68.3	2.0	n/a	n/a	n/a	Bigot-Cormier et al. (1999)
BC3*	7.005	44.358	26.7	0.8	n/a	n/a	n/a	Bigot-Cormier et al. (1999)
BC4*	7.112	44.253	21.2	1.1	n/a	n/a	n/a	Bigot-Cormier et al. (1999)
BC5*	7.164	44.318	20.5	0.7	n/a	n/a	n/a	Bigot-Cormier et al. (1999)
BC6*	7.157	44.304	19.9	0.7	n/a	n/a	n/a	Bigot-Cormier et al. (1999)
BC7*	7.128	44.277	20.9	0.7	n/a	n/a	n/a	Bigot-Cormier et al. (1999)
BC8*	7.135	44.224	25.4	2.2	n/a	n/a	n/a	Bigot-Cormier et al. (1999)
BC9*	7.142	44.204	23.8	1.5	n/a	n/a	n/a	Bigot-Cormier et al. (1999)
BC10*	7.170	44.185	22.9	1.0	n/a	n/a	n/a	Bigot-Cormier et al. (1999)
BC11*	7.160	44.172	27.7	0.9	n/a	n/a	n/a	Bigot-Cormier et al. (1999)
BC12*	7.096	44.175	28.7	1.0	n/a	n/a	n/a	Bigot-Cormier et al. (1999)
BC13*	7.058	44.193	22.1	1.9	n/a	near Isola	n/a	Bigot-Cormier et al. (1999)
BC14*	7.018	44.194	67.2	1.7	n/a	Isola	n/a	Bigot-Cormier et al. (1999)
BC15*	6.920	44.272	59.8	2.3	n/a	St Etienne de Tinee	n/a	Bigot-Cormier et al. (1999)
BC16*	6.891	44.299	57.9	2.5	n/a	n/a	n/a	Bigot-Cormier et al. (1999)
BC17*	7.426	44.189	24.8	1.4	n/a	n/a	n/a	Bigot-Cormier et al. (1999)
BC18*	7.395	44.136	25.1	0.8	n/a	n/a	n/a	Bigot-Cormier et al. (1999)
BC19*	7.371	44.101	25.9	1.1	n/a	n/a	n/a	Bigot-Cormier et al. (1999)
BC20*	7.236	44.084	26.0	1.2	n/a	St Martin de Vesubie	n/a	Bigot-Cormier et al. (1999)
BF1*	6.761	45.677	15.0	n/a	n/a	n/a	n/a	Fuegenschuh et al. (1999)
BF2*	6.771	45.585	22.0	n/a	n/a	n/a	n/a	Fuegenschuh et al. (1999)
BF3*	6.531	45.514	16.0	n/a	n/a	n/a	n/a	Fuegenschuh et al. (1999)
BF4*	6.508	45.343	80.0	n/a	n/a	n/a	n/a	Fuegenschuh et al. (1999)
BF5*	6.504	45.242	89.0	n/a	n/a	n/a	n/a	Fuegenschuh et al. (1999)
BF6*	6.484	45.221	65.0	n/a	n/a	n/a	n/a	Fuegenschuh et al. (1999)
BF7*	6.557	45.195	23.0	n/a	n/a	n/a	n/a	Fuegenschuh et al. (1999)
BF8*	6.551	45.179	78.0	n/a	n/a	n/a	n/a	Fuegenschuh et al. (1999)
BF9*	6.468	45.189	54.0	n/a	n/a	n/a	n/a	Fuegenschuh et al. (1999)
BF10*	6.468	45.174	70.0	n/a	n/a	n/a	n/a	Fuegenschuh et al. (1999)
FT 25A	11.903	46.808	128.4	6.9	n/a	Kofl	n/a	Stoeckhert et al. (1999)
FT 25B	11.908	46.805	119.2	5.5	n/a	Kofl	n/a	Stoeckhert et al. (1999)
FT 26	11.911	46.813	113.2	7.6	n/a	Kofl	n/a	Stoeckhert et al. (1999)
FT 27	11.915	46.810	121.8	7.9	n/a	Kofl	n/a	Stoeckhert et al. (1999)
FT 29	11.852	46.825	40.7	3.3	n/a	Moar	n/a	Stoeckhert et al. (1999)
GE01	11.940	46.852	22.2	1.6	n/a	Uttenheim	n/a	Stoeckhert et al. (1999)
KAW 0065	7.801	46.412	8.9	0.8	310	Tenmatte	n/a	Michalski and Soom (1990)
KAW 0128	8.633	46.735	15.8	1.5	n/a	Gurtnellen	granite	Michalski and Soom (1990)
KAW 0159	8.138	46.196	9.4	1.0	860	Gondo	bt-ms gneiss	Soom (1990)
KAW 0360	8.004	46.342	10.1	0.9	900	Electra	augengneiss	Michalski and Soom (1990)
KAW 0478	8.350	45.986	31.4	1.5	240	Anzola Quarry, Toce Valley	metapelite	Hurford et al. (1991)
KAW 0694	7.053	45.762	25.9	1.9	1390	Aosta Valley, Morgex	gneiss	Hurford et al. (1991)
KAW 1237	9.425	46.581	22.1	1.4	1100	Roffla quarry	n/a	Hunziker et al. (1992)
KAW 1238	9.424	46.596	21.8	1.5	1000	Andeer quarry	n/a	Hunziker et al. (1992)
KAW 1240	9.333	46.505	20.3	1.3	2113	Spluegenpass	n/a	Hunziker et al. (1992)
KAW 1243	9.357	46.418	21.3	1.5	760	Motta	n/a	Hunziker et al. (1992)
KAW 1247	9.357	46.386	18.1	1.2	1020	Prestone, upper quarry	n/a	Hunziker et al. (1992)
KAW 1876	8.063	46.414	10.9	0.5	1060	Val Bavona	gneiss	Hurford (1986)
KAW 1877	8.523	46.452	13.5	0.7	2090	Lago Bianco	gneiss	Hurford (1986)
KAW 1878	8.487	46.319	12.2	0.8	1869	Bosco Gurin	gneiss	Hurford (1986)
KAW 1879	8.578	46.231	15.6	1.0	980	Valle Vergeletto	gneiss	Hurford (1986)
KAW 1880	8.600	46.204	16.1	0.8	960	Valle Onsemone	gneiss	Hurford (1986)
KAW 1881	8.588	46.312	14.2	1.8	680	Linescio	gneiss	Hurford (1986)
KAW 1882	8.697	46.181	14.9	1.2	340	Intragna	gneiss	Hurford (1986)
KAW 1884	8.714	46.240	14.3	0.7	300	Moghegno	gneiss	Hurford (1986)
KAW 1885	8.672	46.280	13.3	0.7	360	Giumaglio Someo	gneiss	Hurford (1986)
KAW 1886	8.621	46.302	13.0	0.9	420	Riveo	gneiss	Hurford (1986)
KAW 1887	8.643	46.360	13.2	1.5	630	Menzonio	gneiss	Hurford (1986)
KAW 1907	6.989	45.944	12.3	1.3	2690	Glacier d'Argentière	bt granite	Soom (1990)
KAW 1914	7.012	45.989	15.7	1.6	3290	Aiguilles du Tour	bt granite	Soom (1990)
KAW 2099	8.700	46.253	13.0	0.7	350	Maggia	gneiss	Hurford (1986)
KAW 2100	8.734	46.219	16.8	0.9	630	Ronchi	gneiss	Hurford (1986)
KAW 2101	8.755	46.190	18.9	0.9	250	Ponte Brolla	pegamtite	Hurford (1986)
KAW 2102	8.726	46.177	18.9	1.5	480	Arcegno	metavolcanic	Hurford (1986)

* unofficial sample number

sample	Longitude degrees east	Latitude degrees north	zircon [Ma]	+/- [Ma]	altitude [m]	Location	lithology	author
KAW 2103	8.751	46.186	18.8	1.2	250	Golino	gneiss	Hurford (1986)
KAW 2104	8.790	46.210	18.0	0.9	1869	Cima della Trosa	gneiss	Hurford (1986)
KAW 2105	8.726	46.141	48.2	3.7	225	Porto Ronco	bedrock	Hurford (1986)
KAW 2207	8.243	46.686	100.0	7.0	720	Guttannen	bt granite gneiss	Michalski and Soom (1990)
KAW 2208	8.306	46.591	12.2	0.6	1350	Handegg	bt granite gneiss	Michalski and Soom (1990)
KAW 2213	8.339	46.565	12.4	0.6	2130	Grimselpass	bt granite gneiss	Michalski and Soom (1990)
KAW 2219	8.321	46.600	13.1	0.7	1586	Chuenzen	bt granite	Michalski and Soom (1990)
KAW 2224	12.084	46.927	27.0	1.2	n/a	Schloss Land	n/a	Stoeckhert et al. (1999)
KAW 2227	11.940	46.841	25.3	1.3	n/a	Uttenheim	n/a	Stoeckhert et al. (1999)
KAW 2228	11.933	46.841	33.8	2.4	n/a	Spitzbach	n/a	Stoeckhert et al. (1999)
KAW 2232	11.978	46.831	94.9	6.8	n/a	Gasthof Sonne	n/a	Stoeckhert et al. (1999)
KAW 2233	11.879	46.825	45.0	2.3	n/a	Platten	n/a	Stoeckhert et al. (1999)
KAW 2234	11.910	46.804	113.2	7.1	n/a	Ried	n/a	Stoeckhert et al. (1999)
KAW 2408	8.304	46.644	15.5	2.0	1200	Tschingelbruecke	granite	Michalski & Soom (1990)
KAW 2417	8.573	45.785	225.0	33.0	330	Angera Ronco	n/a	Giger (1991)
KAW 2461	7.154	45.469	29.5	1.6	1840	Chiapilli	augengneiss	Hurford and Hunziker (1989)
KAW 2462	7.203	45.447	30.0	1.7	1620	Villa	augengneiss	Hurford and Hunziker (1989)
KAW 2463	7.324	45.454	30.0	1.8	1040	Noasca	augengneiss	Hurford and Hunziker (1989)
KAW 2464	7.406	45.442	30.4	1.8	750	Bottegotto	augengneiss	Hurford and Hunziker (1989)
KAW 2471	7.264	45.531	30.4	1.6	4060	Gran Paradiso summit	augengneiss	Hurford and Hunziker (1989)
KAW 2518	8.602	46.676	13.5	1.0	1500	Goeschenen	granite	Michalski & Soom (1990)
KAW 2608	9.407	46.986	96.0	10.0	2400	Schwarze Hoerner	Verrucano	Michalski & Soom (1990)
KAW 2609	9.482	47.048	168.0	16.0	540	Sargans	n/a	Michalski & Soom (1990)
KAW 2612	9.435	46.765	21.3	2.8	630	Rothenbrunnen	marlyschist	Michalski & Soom (1990)
KAW 2616	7.709	46.452	86.9	9.3	1440	Staldi	bt granite	Michalski & Soom (1990)
KAW 2617	7.713	46.314	9.1	0.9	660	Niedergampel	ms gneiss	Soom (1990)
KAW 2618	7.029	46.151	17.2	1.7	460	La Balmaz	migmatitic bt gneiss	Soom (1990)
KAW 2620	9.462	46.225	18.1	1.6	625	Val Codera	granite	Giger (1991)
KAW 2622	9.444	46.229	19.0	1.5	207	Rive Novate	granite	Giger (1991)
KAW 2623	9.698	46.228	22.4	1.9	1855	P. Rossa	n/a	Giger (1991)
KAW 2624	9.682	46.224	21.8	1.9	1600	Val di Sasse Bisolo	n/a	Giger (1991)
KAW 2625	9.653	46.214	22.3	2.1	1025	Val Masino	n/a	Giger(1991)
KAW 2664	7.728	46.405	12.9	1.2	1220	Loetschberg	granite	Michalski & Soom (1990)
KAW 2664	7.728	46.405	12.9	1.2	1220	Loetschbergtunnel-3	granite	Soom (1990)
KAW 2702	7.748	46.425	117.0	12.0	3020	Hockenhorn	bt granite	Soom (1990)
KAW 2726	8.742	45.945	256.0	23.0	440	Brissago	gneiss	Giger (1991)
KAW 2727	8.488	45.791	235.0	21.0	550	Colazza	gneiss	Giger (1991)
KAW 2745	7.476	46.534	181.0	25.0	2100	Rauflihorn	granite boulder	Soom (1990)
KAW 2761	8.094	46.427	11.7	1.1	2870	Eggishorn	bt-ser gneiss	Soom (1990)
KAW 2762	7.635	46.095	35.6	2.9	2080	Petit Mountet	phe augengneiss	Soom (1990)
KAW 2770	8.126	46.166	11.6	1.0	1600	Passo di Monscera-2	bt-ms gneiss	Soom, 1990
KAW 2778	7.550	46.280	25.6	2.9	700	Niouc	chl-ms gneiss	Soom (1990)
KAW 2779	7.602	46.215	23.6	3.0	1580	St. Luc	chl-ms gneiss	Soom (1990)
KAW 2780	7.861	46.349	7.9	0.8	2540	Wiwannihorn	granodiorite	Soom (1990)
KAW 2782	7.867	46.306	8.0	0.8	650	Balmschieder	ser-bt augengneiss	Soom (1990)
KAW 2818	7.504	46.465	94.1	8.8	2040	Hahnenmoos	flysch conglomerate	Soom (1990)
KAW 2983	9.219	46.781	19.2	1.7	700	Ilanz	Verrucano	Soom (1990)
KAW 3120	8.794	46.766	22.4	2.3	2700	Fruttstock	bt-amph-qtz diorite	Michalski & Soom (1990)
KAW 3121	8.805	46.752	27.8	2.3	2240	Brunnibach	bt-plag gneiss	Michalski & Soom (1990)
KAW 3123	8.800	46.795	21.6	2.4	1480	Maderanertal	diatexite	Michalski & Soom (1990)
KAW 3215	9.413	46.914	19.1	4.2	110	Vaettis	mylonite	Michalski & Soom (1990)
KAW 3290	9.829	46.180	23.2	1.9	940	E. Ruvarl / Sandria	n/a	Giger (1991)
KAW 412	7.758	45.914	34.4	3.0	3020	Mezzalama, Valle d'Ayas	gneiss	Hurford et al. (1991)
KAW 414	7.839	45.632	39.7	2.7	660	Lilianes, Gressoney Valley	gneiss	Hurford et al. (1991)
KAW 415	7.918	45.636	32.7	1.9	410	Case Campagnole, Amaz	gneiss	Hurford et al. (1991)
KAW 416	7.748	45.744	33.3	1.8	1150	Arcesa, Valle de Ayas	augengneiss	Hurford et al. (1991)
KAW 417	7.937	45.869	23.8	1.4	1270	Alagna, Val Sesia	gneiss	Hurford et al. (1991)
KAW 473	7.812	45.531	32.7	1.9	250	NW Quassolo, Aosta	gneiss	Hurford et al. (1991)
KAW 474	7.751	45.616	33.0	1.7	380	SE Bard, Aosta	gneiss	Hurford et al. (1991)
KAW 558	7.373	45.841	30.2	1.9	1150	SW Oyace, Valpelline	gneiss	Hurford et al. (1991)
KAW 682	7.519	45.917	30.4	1.8	1950	Prarayer, Valpelline	gneiss	Hurford et al. (1991)
KAW 699	7.951	45.828	27.3	1.9	1250	SW Riva, Val Dobbia	gneiss	Hurford et al. (1991)
KAW 983	7.695	45.954	33.5	1.9	2600	S-face Matterhorn	augengneiss	Hurford et al. (1991)
KAW 987	7.506	45.589	34.5	1.8	1920	Monte Mucrone	gneiss	Hurford et al. (1991)
KAW 989	7.511	45.607	35.3	2.1	1700	Lago Mucrone & Oropa	gneiss	Hurford et al. (1991)
RK 106	11.944	46.890	21.7	1.2	n/a	Muehlen	n/a	Stoeckhert et al. (1999)
RK 81	11.945	46.874	21.0	1.4	n/a	Griesberg	n/a	Stoeckhert et al. (1999)

sample	Longitude degrees east	Latitude degrees north	zircon [Ma]	+/- [Ma]	altitude [m]	Location	lithology	author
RK 92	11.945	46.862	25.2	4.8	n/a	Untergraber	n/a	Stoeckhert et al. (1999)
RS 01	7.357	46.219	22.9	3.2	500	n/a	n/a	Seward and Mancktelow (1994)
RS 03	7.230	46.157	25.9	5.2	1280	n/a	n/a	Seward and Mancktelow (1994)
RS 04	7.074	46.091	11.4	2.0	730	n/a	n/a	Seward and Mancktelow (1994)
RS 21	6.676	45.746	10.6	1.6	760	n/a	n/a	Seward and Mancktelow (1994)
RS 39	7.166	46.093	13.4	3.0	1740	n/a	n/a	Seward and Mancktelow (1994)
RS 40	7.176	46.094	16.3	3.5	1080	n/a	n/a	Seward and Mancktelow (1994)
RS 42	7.157	46.081	13.5	1.8	725	n/a	n/a	Seward and Mancktelow (1994)
RS 46	7.228	46.088	19.7	3.1	1400	n/a	n/a	Seward and Mancktelow (1994)
RS 47	7.216	46.090	17.7	4.6	1140	n/a	n/a	Seward and Mancktelow (1994)
RS 49	7.127	46.084	11.2	2.5	930	n/a	n/a	Seward and Mancktelow (1994)
RS 65	7.116	45.889	17.0	3.2	2230	n/a	n/a	Seward and Mancktelow (1994)
Gi 462	9.249	46.125	210.0	84.0	n/a	n/a	n/a	Bertotti et al. (1999)
Gi 468	9.384	46.130	49.4	7.4	n/a	n/a	n/a	Bertotti et al. (1999)
DB 9016	9.306	46.053	151.0	31.0	n/a	n/a	n/a	Bertotti et al. (1999)
DB 9020	9.244	46.041	176.0	29.0	n/a	n/a	n/a	Bertotti et al. (1999)
Gi 366	9.347	46.066	161.0	28.0	n/a	n/a	n/a	Bertotti et al. (1999)
Gi 367	9.347	46.066	144.0	15.0	n/a	n/a	n/a	Bertotti et al. (1999)
Gi 368	9.347	46.066	135.0	14.0	n/a	n/a	n/a	Bertotti et al. (1999)
Gi 371	9.353	46.049	177.0	34.0	n/a	n/a	n/a	Bertotti et al. (1999)
Gi 372	9.338	46.043	223.0	40.0	n/a	n/a	n/a	Bertotti et al. (1999)
Gi 374	9.330	46.089	139.0	28.0	n/a	n/a	n/a	Bertotti et al. (1999)
V302	7.251	45.321	32.7	n/a	1280	Molette	meta Fe-gabbro	Vance (1999)
V304	7.424	45.170	33.4	n/a	1000	Val della Torre	plagiogranite	Vance
V342	7.718	45.637	28.2	n/a	380	Echallod-Inf.	metatrondhjemite dike	Vance
V344	7.787	45.591	35.8	n/a	300	Pont St. Martin	metaaplite	Vance
V345	7.533	45.414	32.2	n/a	550	Sparone	gneiss	Vance
V346	7.430	45.885	30.1	n/a	1800	Bionaz	gneiss?	Vance
V348	7.487	46.034	35.9	n/a	1990	Arolla	gneiss	Vance
V361	7.180	45.886	31.5	n/a	2100	Colle de Gran S. Bernardo	aplitic gneiss	Vance
V362	6.971	45.145	30.1	n/a	1100	Pra Piano	metaaplite?	Vance
V363	7.290	45.644	24.6	n/a	1300	pte dl Laval	metaquartz diorite	Vance
V364	7.193	45.985	29.5	n/a	1346	Liddes	phyllonitic gneiss	Vance
V366	7.142	45.609	30.8	n/a	1400	Meglion - Frassiney	schistose quartzite	Vance
V382	7.280	44.205	16.9	n/a	1400	Terme di Valderi	granite	Vance
V384	7.272	45.449	29.2	n/a	1500	Ceresole Reale	gneiss	Vance
V385	7.392	45.598	33.3	n/a	1600	Lillaz	gneiss	Vance
V386	7.503	45.504	32.2	n/a	1050	Lasinetto	gneiss	Vance
V387	7.742	45.521	27.1	n/a	827	Traversella -1	granite dike	Vance
V391	7.303	45.118	30.5	n/a	380	Condove	porphyritic granite	Vance
V393	7.201	44.684	26.8	n/a	904	Crissolo - Paesana	gneiss	Vance
V394	7.372	44.569	22.9	n/a	600	Venasca	porphyritic granite	Vance
V400	7.275	44.174	19.5	n/a	1500	Terme dl Valderi	granite	Vance
V413	7.293	44.226	19.1	n/a	1300	Terme di Valderi	migmatitic gneiss	Vance
V424	7.856	45.501	135.0	n/a	250	Borgofranco di Ivrea	granite (di Monalto)	Vance (1999)
V425	7.824	45.478	135.0	n/a	270	Lessolo	granite (di Fiorano)	Vance (1999)
V426	7.887	45.499	123.0	n/a	400	Chiaverano	granitic granulite	Vance (1999)
V522	6.654	45.190	34.6	n/a	1000	Modane	gneiss, porphyritic grai	Vance
V524	6.114	45.210	15.2	n/a	1500	Belledonne	leucogneiss	Vance
V531	6.733	44.904	87.3	n/a	2640	M. Gimoni	albitite, syenite dike	Vance
V533	7.360	44.625	25.1	n/a	500	Martiniana Po	coesite locality	Vance
V534	7.207	44.925	29.7	n/a	700	Torre Pellice	gneiss (di Luserna)	Vance
V535	7.346	44.511	28.9	n/a	1614	C.dl Valmala	schistose gneiss	Vance
V536	7.269	44.421	28.2	n/a	822	Pradleves	leucogneiss - quartzite	Vance
V537	7.105	44.313	20.1	n/a	1000	Pianche	gneiss	Vance
V538	6.998	44.342	20.0	n/a	1600	M. Bassura	orthogneiss	Vance
V539	6.948	44.448	169.4	n/a	2500	Acceglio	Quartzite	Vance
V541	7.840	45.113	163.0	n/a	270	Colline di Torino	hbl-biotite tonalite	Vance
V543	7.671	45.395	191.0	n/a	375	Cuorgne	granite	Vance (1999)
V544	7.623	45.361	128.0	n/a	400	Valperga (Belmonte)	granite	Vance (1999)
V546	7.594	45.338	136.0	n/a	420	Levone	granite	Vance (1999)
V547	7.874	45.481	115.0	n/a	240	Cascinette di Ivrea	granitoid dike	Vance (1999)
V548	8.279	45.803	146.0	n/a	800	Rocca Pietra	biotite granitoid	Vance (1999)
V549	8.274	45.715	149.0	n/a	354	Borgosesia	biotite granitoid	Vance (1999)
V619	8.265	45.698	167.9	n/a	370	Crevacuore	Permian Tuff	Vance (1999)
V621	7.925	44.311	31.1	n/a	600	Costa Dardella	orthogneiss	Vance (1999)
V622	8.067	44.211	179.1	n/a	630	Calizzano	orthogneiss	Vance (1999)

Bertotti cited at 2SE

V388 is mis-labeled here as V387

V387 V388

sample	Longitude degrees east	Latitude degrees north	zircon [Ma]	+/- [Ma]	altitude [m]	Location	lithology	author
V623	8.066	44.352	30.6	n/a	400	Nucetto	augengneiss	Vance (1999)
V624	8.473	44.367	124.3	n/a	72	Savona	augengneiss	Vance (1999)
V625	8.527	44.606	31.6	n/a	574	Valosio	augengneiss	Vance (1999)
V626	8.460	45.926	197.7	n/a	196	Baveno	granite	Vance (1999)
V627	8.362	45.796	186.7	n/a	370	Alzo	granite	Vance (1999)
V628	8.173	45.587	185.6	n/a	330	Granito del Biellese	granite	Vance (1999)
V629	8.010	45.584	27.0	n/a	330	Biella	n/a	Vance (1999)
V630	8.005	45.565	26.4	n/a	530	Biella	n/a	Vance (1999)
V648	8.115	44.278	31.3	n/a	900	Barbissira	gneiss	Vance (1999)
V650	8.235	44.100	31.1	n/a	180	Pietra Ligure	n/a	Vance (1999)
V651	8.347	44.333	136.0	n/a	250	Altare	n/a	Vance (1999)
V654	8.296	45.937	77.8	n/a	850	Valstrona	stronalite	Vance
V658	7.053	45.361	29.5	n/a	1819	Bonneval	gneiss Minuti	Vance
V659	6.269	45.047	20.0	n/a	?	Le Chazlet	granitoid Pelvoux	Vance

References for data repository:

Bertotti, G., Seward, D., Wibrans, J., ter Voorde, M., and Hurford, A. J., 1999, Crustal thermal regime prior to, during , and after rifting: A geochronological and modeling study of the Mesozoic South Alpine rifted margin: Tectonics, v. 18, p. 185-200.

Bigot-Cormier, F. Poupeau, G., Sosson, M., Stéphan, J.-F., Labrin, E., Ziad, N., and Schwartz, S., 1999, Fission track record and exhumation rates of the Argentera external crystalline massif: Memoire di Siencze Geologiche, v. 51, p. 17-19.

Fügenschuh, B., Loprieno, A., Ceriani, S., and Schmid, S. M., 1999, Structural analysis of the Subbriabçonnais and Valais units in the area of Moûtiers (Savoy, Western Alps): paleaogeographic and tectonic consequences: International Journal of Earth Sciences, 88, p. 201-218.

Giger, M., 1991, Geochronologische und petrographische Studien an Geröllen und Sedimenten der Gonfolite Lombarda Gruppe (Südschweiz und Norditalien) und ihr Vergleich mit dem alpinen Hinterland. Ph.D thesis, University of Berne, Berne; Switzerland, 227p., (unpublished).

Giger, M., and Hurford, A. J., 1989, Tertiary intrusives of the Central Alps: Their Tertiary uplift, erosion, redeposition and burial in the south-alpine foreland: Eclogae Geologicae Helvetiae, v. 82/3, p. 857-866.

Hunziker, J. C., Desmond, J., and Hurford, A. J., 1992, Thirty-two years of geochronological work in the Central and Western Alps: A review on seven maps: Memoir De Geologie (Lausanne) 13, p. 1-59.

Hurford, A. J., 1986, Cooling and uplift patterns in the Lepontine Alps South Central Switzerland and an age of vertcal movement on the Insubric fault line: Contributions to Mineralogy and Petrology, v. 92, p. 413-427.

Hurford, A. J., and Hunziker, J.C., 1989, A revised thermal history for the Gran Paradiso massif: Schweizerische Mineralogische und Petrographische Mitteilungen. v. 69, p. 319-329.

Hurford, A. J., Hunziker, J. C., and Stöckhert, B., 1991, Constraints on the late thermotectonic evolution of the Western Alps: Evidence for episodic rapid uplift: Tectonics, v. 10, p. 758-769.

Lihou, J. C., Hurford, A. J., and Carter, A., 1995, Preliminary fission-track ages on zircons and apatites from the Sardona unit, Glarus Alps, eastern Switzerland:

late Miocene-Pliocene exhumation rates: Schweizerische Mineralogische und Petrographische Mitteilungen. v. 75, p. 177-186.

Michalski, I., and Soom, M., 1990, The Alpine thermo-tectonic evolution of the Aar and Gotthard massifs, Central Switzerland: Fission track ages on zircon and apatite and K-Ar mica ages: Schweizerische Mineralogische und Petrographische Mitteilungen, v. 70, p. 373-387.

Soom, M., 1990, Abkühlungs- und Hebungsgeschichte der Extemmassive und der penninischen Decken beidseits der Simplon-Rhône-Linie seit dem Oligozän: Spaltspurdatierungen an Apatit/Zirkon und K-Ar-Datierungen an Biotit/Muskowit (Westliche Zentralalpen): PhD-thesis, University of Bern. Unpublished.

Stöckhert, B., Brix, M. R., Kleinschrodt, R., Hurford, A. J., and Wirth, R., 1999, Thermochronometry and microstructures of quartz – a comparison with experimental flow laws and predictions on the temperature of brittle-plastic transition: Journal of Structural Geology, v. 21, p. 351-369.

Vance, J., 1999, Zircon fission track evidence for a Jurassic (Tethyan) thermal event in the Western Alps: Memorie di Scienze Geologiche, v. 51, p. 473-476.